International Journal of Neural Systems, Vol. 17, No. 2 (2007) 71–78

World Scientific
www.worldscientific.com

GRANGER CAUSALITY BETWEEN MULTIPLE INTERDEPENDENT NEUROBIOLOGICAL TIME SERIES: BLOCKWISE VERSUS PAIRWISE METHODS

XUE WANG
J. Crayton Pruitt Family Department of Biomedical Engineering, University of Florida, 121 BME Building, Gainesville, FL 32611, USA

YONGHONG CHEN
J. Crayton Pruitt Family Department of Biomedical Engineering, University of Florida, 102B BME Building, Gainesville, FL 32611, USA

STEVEN L. BRESSLER
Center for Complex Systems and Brain Sciences, Florida Atlantic University, Boca Raton, FL 33431, USA

MINGZHOU DING
J. Crayton Pruitt Family Department of Biomedical Engineering, University of Florida, 149 BME Building, Gainesville, FL 32611, USA
mding@bme.ufl.edu
www.ufl.edu

Granger causality is becoming an important tool for determining causal relations between neurobiological time series. For multivariate data, there is often the need to examine causal relations between two blocks of time series, where each block could represent a brain region of interest. Two alternative methods are available. In the pairwise method, bivariate autoregressive models are fit to all pairwise combinations involving one time series from the first block and one from the second. The total Granger causality between the two blocks is then derived by summing pairwise causality values from each of these models. This approach is intuitive but computationally cumbersome. Theoretically, a more concise method can be derived, which we term the blockwise Granger causality method. In this method, a single multivariate model is fit to all the time series, and the causality between the two blocks is then computed from this model. We compare these two methods by applying them to cortical local field potential recordings from monkeys performing a sensorimotor task. The obtained results demonstrate consistency between the two methods and point to the significance potential of utilizing Granger causality analysis in understanding coupled neural systems.

Keywords: Multivariate time series; pairwise Granger causality; blockwise Granger causality; sensorimotor cortex, beta oscillation network.

1. Introduction

The issue of determining directionality in neural interactions has become a focus of strong interest in neuroscience since directionality holds the promise of revealing paths of information flow within the nervous system. In this regard, Granger causality and its spectral counterpart have emerged as the leading statistical quantities to furnish directional information from multivariate neural data. The concept of Granger causality[1,2] follows directly from consideration of two time series. If the first time series is better predicted by its past measurements in conjunction with those of the second time series than by its own past values alone, then the second time series is said to be causal to the first time series. The roles of the two time series can be reversed to address the causal influence in the opposite direction. Granger causality

can also be studied in the frequency domain. In fact, Geweke's[3] frequency decomposition of the time domain Granger causality, which allows the examination of causal relations among oscillatory neural activities, is the focus of the present work.

Granger causality had its genesis in the economics field, and its deployment in neuroscience has only begun fairly recently.[4–8] Applications to the investigation of causal influences between different brain structures have so far mainly utilized pairwise analysis[9,10] in which two time series are analyzed at a time. However, pairwise analysis may be considered inadequate given the rapid advances that have occurred in multi-site recording technology in recent years. When dealing with large sets of multivariate neural time series data, a more sensible approach for many purposes is to combine the time series recorded from different brain regions of interest into blocks, and then to analyze the relations between the blocks. Although it is possible to achieve a blockwise analysis by combining the results of repeated pairwise analyses, a more effective, and theoretically more elegant, approach is to address the relation between two blocks of time series directly. This blockwise approach is contained in the general methodological framework developed by Geweke.[3] In what follows, we first introduce the mathematical framework for deriving Granger causality between two blocks of time series (Sec. 2). We then compare the performance of this blockwise method with that of the bivariate approach by applying both to multi-site local field potential recordings from the cerebral cortex of monkeys performing sensorimotor tasks (Sec. 3). For this comparison study, one block is defined to contain a single time series and the remaining time series in the data set comprise the other block. Section 4 summarizes the work.

2. Methods

2.1. *Time domain formulation*

In what follows, boldface letters with an arrow on top denote vectors and boldface letters without arrows denote matrices. The formulation below follows that of Geweke[3] and Chen *et al.*[11] Let $\vec{\mathbf{W}}_t = [w_{1t}, w_{2t}, \ldots, w_{pt}]'$ be a multivariate stationary process with dimension p, where the prime denotes the matrix transposition. Under fairly general conditions, $\vec{\mathbf{W}}_t$ could be represented by the following multivariate autoregressive (MVAR) model:

$$\vec{\mathbf{W}}_t = \sum_{i=1}^{\infty} \mathbf{a}_i \, \vec{\mathbf{W}}_{t-i} + \vec{\varepsilon}_t. \tag{1}$$

Suppose that $\vec{\mathbf{W}}_t$ was partitioned into two vectors $\vec{\mathbf{X}}_\mathbf{t}$ and $\vec{\mathbf{Y}}_\mathbf{t}$ with dimensions k and l: $\vec{\mathbf{W}}_\mathbf{t} = \left(\vec{\mathbf{X}}'_t, \vec{\mathbf{Y}}'_t\right)$, where $k + l = p$. In the case of pairwise Granger causality, $\vec{\mathbf{X}}_\mathbf{t}$ and $\vec{\mathbf{Y}}_\mathbf{t}$ are two one-dimension time series ($k = 1, l = 1$); while in the case of blockwise Granger causality, $\vec{\mathbf{X}}_\mathbf{t}$ and $\vec{\mathbf{Y}}_\mathbf{t}$ are two sets of time series of dimensions k and l typically not equal to 1. ($\vec{\mathbf{X}}_\mathbf{t}$ and $\vec{\mathbf{Y}}_\mathbf{t}$ have no overlap.)

Individually, $\vec{\mathbf{X}}_\mathbf{t}$ and $\vec{\mathbf{Y}}_\mathbf{t}$ can each be represented by the following models

$$\begin{aligned} \vec{\mathbf{X}}_t &= \sum_{j=1}^{\infty} \mathbf{a}_{1j} \; \vec{\mathbf{X}}_{t-j} + \vec{\varepsilon}_{1t}, \quad \text{var}\,(\vec{\varepsilon}_{1t}) = \Sigma_1 \\ \vec{\mathbf{Y}}_t &= \sum_{j=1}^{\infty} \mathbf{d}_{1j} \; \vec{\mathbf{Y}}_{t-j} + \vec{\boldsymbol{\eta}}_{1t}, \quad \text{var}\,(\vec{\boldsymbol{\eta}}_{1t}) = \boldsymbol{\Gamma}_1. \end{aligned} \tag{2}$$

Jointly, they are represented as

$$\begin{aligned} \vec{\mathbf{X}}_t &= \sum_{j=1}^{\infty} \mathbf{a}_{2j} \; \vec{\mathbf{X}}_{t-j} + \sum_{j=1}^{\infty} \mathbf{b}_{2j} \, \vec{\mathbf{Y}}_{t-j} + \vec{\varepsilon}_{2t} \\ \vec{\mathbf{Y}}_t &= \sum_{j=1}^{\infty} \mathbf{c}_{2j} \; \vec{\mathbf{X}}_{t-j} + \sum_{j=1}^{\infty} \mathbf{d}_{2j} \; \vec{\mathbf{Y}}_{t-j} + \vec{\boldsymbol{\eta}}_{2t}. \end{aligned} \tag{3}$$

where $\vec{\varepsilon}_{2t}$ and $\vec{\boldsymbol{\eta}}_{2t}$ are uncorrelated over time within themselves and with each other, but could be correlated with each other at the same time and their contemporaneous covariance matrix is

$$\boldsymbol{\Sigma} = E\left(\begin{pmatrix} \vec{\varepsilon}_{2t} \\ \vec{\boldsymbol{\eta}}_{2t} \end{pmatrix} (\vec{\varepsilon}_{2t} \quad \vec{\boldsymbol{\eta}}_{2t})\right) = \begin{pmatrix} \boldsymbol{\Sigma}_2 & \boldsymbol{\Upsilon}_2 \\ \boldsymbol{\Upsilon}'_2 & \boldsymbol{\Gamma}_2 \end{pmatrix}. \tag{4}$$

Notice that Eq. (3) actually is the partitioned form of Eq. (1). The total interdependence between $\vec{\mathbf{X}}_t$ and $\vec{\mathbf{Y}}_t$ is defined as

$$F_{\mathbf{X},\mathbf{Y}} = \ln \frac{|\Sigma_1||\Gamma_1|}{|\Sigma|} \tag{5}$$

where $|\cdot|$ denotes the determinant of the enclosed matrix. When $\vec{\mathbf{X}}_t$ and $\vec{\mathbf{Y}}_t$ are independent, $F_{\mathbf{X},\mathbf{Y}} = 0$. The total interdependence $F_{\mathbf{X},\mathbf{Y}}$ between two sets of

time series $\vec{\mathbf{X}}_t$ and $\vec{\mathbf{Y}}_t$ can be decomposed into three components.

$$F_{\mathbf{X},\mathbf{Y}} = F_{\mathbf{X}\to\mathbf{Y}} + F_{\mathbf{Y}\to\mathbf{X}} + F_{\mathbf{X}\cdot\mathbf{Y}}. \tag{6}$$

where

$$F_{\mathbf{Y}\to\mathbf{X}} = \ln\frac{|\Sigma_1|}{|\Sigma_2|} \tag{7}$$

$$F_{\mathbf{X}\to\mathbf{Y}} = \ln\frac{|\Gamma_1|}{|\Gamma_2|} \tag{8}$$

are the linear causality from $\vec{\mathbf{Y}}_t$ to $\vec{\mathbf{X}}_t$ and from $\vec{\mathbf{X}}_t$ to $\vec{\mathbf{Y}}_t$ due to their interactions. And

$$F_{\mathbf{X}\cdot\mathbf{Y}} = \ln\frac{|\Sigma_2||\Gamma_2|}{|\Sigma|} \tag{9}$$

is the instantaneous causality.

2.2. *Frequency domain formulation*

To examine the directional linear causality relations in the frequency domain, Eq. (3) is rewritten into the following form with the lag operator $L(L\,\vec{\mathbf{X}}_t = \vec{\mathbf{Y}}_{t-1})$

$$\begin{pmatrix}\mathbf{B}_{xx}(L) & \mathbf{B}_{xy}(L)\\ \mathbf{B}_{yx}(L) & \mathbf{B}_{yy}(L)\end{pmatrix}\begin{pmatrix}\vec{\mathbf{X}}_t\\ \vec{\mathbf{Y}}_t\end{pmatrix} = \begin{pmatrix}\vec{\varepsilon}_{2t}\\ \vec{\boldsymbol{\eta}}_{2t}\end{pmatrix} \tag{10}$$

where

$$\begin{aligned}
\mathbf{B}_{xx}(L) &= \mathbf{I}_k - \sum_{j=1}^{\infty}\mathbf{a}_{2j}L^j,\\
\mathbf{B}_{xy}(L) &= -\sum_{j=1}^{\infty}\mathbf{b}_{2j}L^j,\\
\mathbf{B}_{yx}(L) &= -\sum_{j=1}^{\infty}\mathbf{c}_{2j}L^j,\\
\mathbf{B}_{yy}(L) &= \mathbf{I}_l - \sum_{j=1}^{\infty}\mathbf{d}_{2j}L^j, \quad \text{and}\\
\mathbf{B}_{xx}(0) &= \mathbf{I}_k, \quad \mathbf{B}_{yy}(0) = \mathbf{I}_l,\\
\mathbf{B}_{xy}(0) &= \mathbf{0}, \quad \mathbf{B}_{yx}(0) = \mathbf{0}.
\end{aligned}$$

By pre-multiplying a transformation matrix $\mathbf{P}$ to both sides of Eq. (10)

$$\mathbf{P} = \begin{pmatrix}\mathbf{I}_k & \mathbf{0}\\ -\boldsymbol{\Upsilon}_2'\Sigma_2^{-1} & \mathbf{I}_l\end{pmatrix} \tag{11}$$

we can get the following equation:

$$\begin{pmatrix}\mathbf{B}_{xx}(L) & \mathbf{B}_{xy}(L)\\ \tilde{\mathbf{B}}_{yx}(L) & \tilde{\mathbf{B}}_{yy}(L)\end{pmatrix}\begin{pmatrix}\vec{\mathbf{X}}_t\\ \vec{\mathbf{Y}}_t\end{pmatrix} = \begin{pmatrix}\vec{\varepsilon}_{2t}\\ \vec{\tilde{\eta}}_{2t}\end{pmatrix} \tag{12}$$

where

$$\tilde{\mathbf{B}}_{yx}(L) = \mathbf{B}_{yx} - \boldsymbol{\Upsilon}_2'\Sigma_2^{-1}\mathbf{B}_{xx}(L),$$

$$\tilde{\mathbf{B}}_{yy}(L) = \mathbf{B}_{yy} - \boldsymbol{\Upsilon}_2'\Sigma_2^{-1}\mathbf{B}_{xy}(L),$$

$$\vec{\tilde{\eta}}_{2t} = \vec{\boldsymbol{\eta}}_{2t} - \boldsymbol{\Upsilon}_2'\Sigma_2^{-1}\,\vec{\varepsilon}_{2t}.$$

Now $\vec{\varepsilon}_{2t}$ and $\vec{\tilde{\eta}}_{2t}$ are uncorrelated with each other even at the same time,

$$\begin{aligned}
\operatorname{cov}(\vec{\varepsilon}_{2t}, \vec{\tilde{\eta}}_{2t}) &= 0,\\
\operatorname{var}(\vec{\tilde{\eta}}_{2t}) &= \tilde{\Gamma}_2 = \Gamma_2 - \boldsymbol{\Upsilon}_2'\Sigma_2^{-1}\boldsymbol{\Upsilon}_2.
\end{aligned}$$

The covariance matrix of the noise terms is

$$\tilde{\Sigma} = E\left(\begin{pmatrix}\vec{\varepsilon}_{2t}\\ \vec{\tilde{\eta}}_{2t}\end{pmatrix}\begin{pmatrix}\vec{\varepsilon}_{2t} & \vec{\tilde{\eta}}_{2t}\end{pmatrix}\right) = \begin{pmatrix}\Sigma_2 & \mathbf{0}\\ \mathbf{0} & \tilde{\Gamma}_2\end{pmatrix}. \tag{13}$$

Taking the Fourier transform of both sides of Eq. (12) leads to

$$\begin{pmatrix}\mathbf{B}_{xx}(\omega) & \mathbf{B}_{xy}(\omega)\\ \tilde{\mathbf{B}}_{yx}(\omega) & \tilde{\mathbf{B}}_{yy}(\omega)\end{pmatrix}\begin{pmatrix}\vec{\mathbf{X}}_t(\omega)\\ \vec{\mathbf{Y}}_t(\omega)\end{pmatrix} = \begin{pmatrix}\vec{\mathbf{E}}_x(\omega)\\ \vec{\tilde{\mathbf{E}}}_y(\omega)\end{pmatrix} \tag{14}$$

Defining transfer function $\tilde{\mathbf{H}}$ as the inverse of the coefficient matrix $\tilde{\mathbf{B}}$ and $\mathbf{B}$, we can get

$$\begin{pmatrix}\vec{\mathbf{X}}(\omega)\\ \vec{\mathbf{Y}}(\omega)\end{pmatrix} = \begin{pmatrix}\tilde{\mathbf{H}}_{xx}(\omega) & \tilde{\mathbf{H}}_{xy}(\omega)\\ \tilde{\mathbf{H}}_{yx}(\omega) & \tilde{\mathbf{H}}_{yy}(\omega)\end{pmatrix}\begin{pmatrix}\vec{\mathbf{E}}_x(\omega)\\ \vec{\tilde{\mathbf{E}}}_y(\omega)\end{pmatrix} \tag{15}$$

The spectral matrix is then

$$\mathbf{S}(\omega) = \begin{pmatrix}\mathbf{S}_{xx}(\omega) & \mathbf{S}_{xy}(\omega)\\ \mathbf{S}_{yx}(\omega) & \mathbf{S}_{yy}(\omega)\end{pmatrix} = \tilde{\mathbf{H}}(\omega)\tilde{\Sigma}\tilde{\mathbf{H}}^*(\omega) \tag{16}$$

where $\mathbf{S}_{xy}(\omega) = \mathbf{S}_{yx}^*(\omega)$ with $*$ denoting complex conjugate and matrix transposition.

The total interdependence between $\vec{\mathbf{X}}_\mathbf{t}$ and $\vec{\mathbf{Y}}_\mathbf{t}$ in the frequency domain is defined as

$$f_{\mathbf{X},\mathbf{Y}} = \ln\frac{|\mathbf{S}_{xx}(\omega)||\mathbf{S}_{yy}(\omega)|}{|\mathbf{S}(\omega)|}. \tag{17}$$

Equations (13) and (16) imply the following spectral decomposition of the spectral density of $\vec{\mathbf{X}}_t$

$$\mathbf{S}_{xx}(\omega) = \tilde{\mathbf{H}}_{xx}(\omega)\Sigma_2\tilde{\mathbf{H}}_{xx}^*(\omega) + \tilde{\mathbf{H}}_{xy}(\omega)\tilde{\Gamma}_2\tilde{\mathbf{H}}_{xy}^*(\omega). \tag{18}$$

The first term in Eq. (18) can be interpreted as the intrinsic power of $\vec{\mathbf{X}}_\mathbf{t}$ and the second term as the causal power of $\vec{\mathbf{X}}_\mathbf{t}$ due to $\vec{\mathbf{Y}}_\mathbf{t}$. This interpretation suggests the definition of the causal influence from $\vec{\mathbf{Y}}_\mathbf{t}$ to $\vec{\mathbf{X}}_\mathbf{t}$ at frequency ω as

$$f_{\mathbf{Y}\to\mathbf{X}}(\omega) = \ln\frac{|\mathbf{S}_{xx}(\omega)|}{|\tilde{\mathbf{H}}_{xx}(\omega)\Sigma_2\tilde{\mathbf{H}}_{xx}^*(\omega)|} \tag{19}$$

Using $\begin{pmatrix} \mathbf{I}_k & -\boldsymbol{\Upsilon}_2\Gamma_2^{-1} \\ \mathbf{0} & \mathbf{I}_l \end{pmatrix}$ as the transformation matrix and following the same steps that lead to Eq. (19), we get the causal influence from $\vec{\mathbf{X}}_\mathbf{t}$ to $\vec{\mathbf{Y}}_\mathbf{t}$ at frequency ω:

$$f_{\mathbf{X}\to\mathbf{Y}}(\omega) = \ln \frac{|\mathbf{S}_{yy}(\omega)|}{|\tilde{\mathbf{H}}_{yy}(\omega)\Gamma_2\tilde{\mathbf{H}}^*_{yy}(\omega)|}. \tag{20}$$

By defining the instantaneous causality in the spectral domain as[12]

$$f_{\mathbf{X}\cdot\mathbf{Y}}(\omega) = \ln \frac{|(\tilde{\mathbf{H}}_{xx}(\omega)\Sigma_2\tilde{\mathbf{H}}^*_{xx}(\omega))||(\tilde{\mathbf{H}}_{yy}(\omega)\Gamma_2\tilde{\mathbf{H}}^*_{yy}(\omega))|}{|\mathbf{S}(\omega)|}, \tag{21}$$

we achieve frequency domain decomposition for the total interdependence as,

$$f_{\mathbf{X},\mathbf{Y}}(\omega) = f_{\mathbf{Y}\to\mathbf{X}}(\omega) + f_{\mathbf{X}\to\mathbf{Y}}(\omega) + f_{\mathbf{X}\cdot\mathbf{Y}}(\omega). \tag{22}$$

Notice that Eq. (22) is the frequency domain counterpart of Eq. (6).

For two time series, we simply let $p = 2, l = 1$ and $k = 1$, and call the approach the pairwise (bivariate) approach. When the data set can be sensibly divided into two blocks, one can fit one MVAR model to the data by a method proposed in Ding *et al.*[13] The interdependencies are then estimated by Eqs. (19)–(21).

3. Applications to Cortical Local Field Potential Data

Local field potential data were recorded from two macaque monkeys using transcortical bipolar electrodes chronically implanted at distributed sites in multiple cortical areas of one hemisphere (right hemisphere in monkey GE and left hemisphere in monkey LU) while the monkeys performed a GO/NO-GO visual pattern discrimination task.[14] Figure 1 shows the electrode placement. The presence of oscillatory field potential activity in the beta (14–30 Hz) frequency range was recently reported in the sensorimotor cortex of these monkeys during the prestimulus period when the monkey maintained steady pressure on a mechanical lever and paid attention to the computer screen anticipating the imminent onset of the visual stimulus.[10] In that study, Granger causality analysis was performed for all pairwise combinations of sensorimotor cortical recording sites indicated by the heavy circles in Fig. 1.

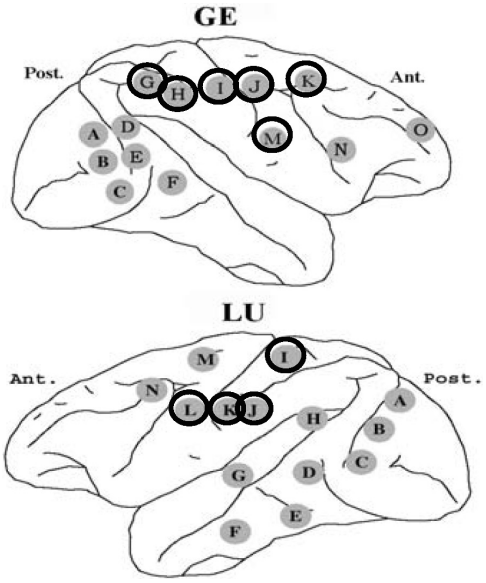

Fig. 1. Locations of recording sites. The sites enclosed by the heavy circles are the sites involved in the beta oscillation network in the sensorimotor cortex.

In both monkeys, a network of sensorimotor sites was found to be coherent (synchronized) in the beta frequency range in relation to maintenance of the depressed mechanical lever. Within this network, significant beta-frequency Granger causal influences were discovered from primary somatosensory cortex to both primary motor cortex and inferior posterior parietal cortex, with the latter area also exerting Granger causal influences on primary motor cortex.

In a pairwise analysis, the values of peak beta-frequency Granger causality between the primary somatosensory cortex site (I in GE and K in LU) and all other sites with which it was coherent in the beta frequency range were summed. The summed (outgoing) influence exerted by the primary somatosensory cortex site on the other sites was 5.9 times larger in GE than the summed (incoming) influence that the other sites exerted on it, and 5.2 times larger in LU. In contrast, the summed incoming influence for the primary motor cortex site (site L in LU) was 4.1 times larger than the summed outgoing influence in LU, and in GE only the incoming influences for the primary motor cortex site (site J in GE) were statistically significant. The primary somatosensory cortex site thus appeared to be a major source of influence in the beta frequency range for the other network sites, whereas the precentral motor sites appeared

to be a major receiving site from the other network sites.

The above study makes it abundantly clear that the functional relation between one recording site and the rest of the network can be useful for assessing the relative importance of that site in organizing the dynamics of the network. It thus appears that the blockwise Granger causality method might be ideally suited for addressing this functional relation if we treat one time series as a block and the remaining time series as another. That is why we have re-analyzed the same data with the blockwise Granger causality method in order to compare the summed pairwise and blockwise methods for assessing Granger causality between one recording site and the rest of the network. The results obtained from both methods are presented for monkey GE in Fig. 2 and LU in Fig. 3.

In Figs. 2 and 3, the solid curves result from the blockwise Granger causality method in the frequency domain (Eqs. 19 and 20 with $k = 1$ and $l = 6$) and the dashed curves are from the summed pairwise Granger causality method ($k = 1, l = 1$). For instance, the outgoing summed pairwise Granger causality from site J (i.e., $J \rightarrow$ remaining sites) is the sum of the pairwise Granger causality values from J to each of the other sites (i.e., $J \rightarrow I + J \rightarrow G + J \rightarrow K + J \rightarrow M + J \rightarrow H$). As can be seen, the results from both methods are similar in terms of the shape of the Granger causality spectra and the peak locations in the entire spectrum (0–100 Hz). The peak values from the blockwise method tend to be slightly smaller compared with the summed peak values from the pairwise method.

In Fig. 3, for demonstration purposes, we have also included Granger causality spectra (solid thick curves) estimated between the individual time series of one site and the average time series computed from the block of multiple time series of the other sites (that is $k = 1$ and $l = 1$ here too). This comparison is included since in many studies, the time series from a given region-of-interest (ROI) are averaged before assessing functional relations among the ROIs. Once the average of all the rest of time series

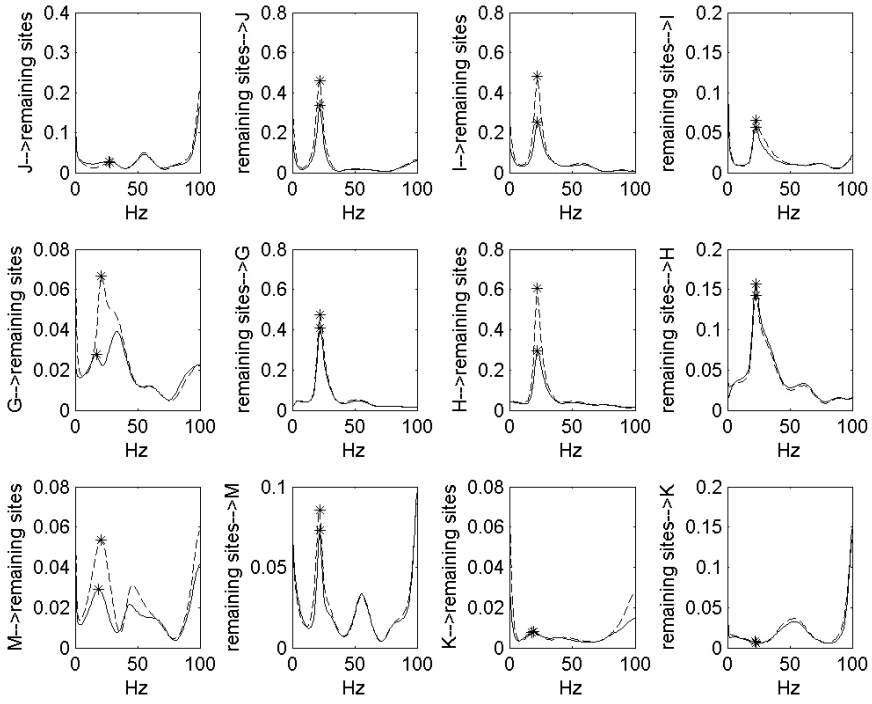

Fig. 2. Blockwise Granger causality (solid) and summed pairwise Granger causality (dashed) for the beta-coherent network of monkey GE. Here, "$X \rightarrow$ remaining sites" denotes the outgoing causality exerted by site X on the other sites in the network, and "remaining sites $\rightarrow X$" denotes the incoming causality from the other sites to X, where X represents site G, H, I, J, K, or M. The stars indicate the peaks of the Granger causality spectra within the beta (14–30 Hz) frequency range.

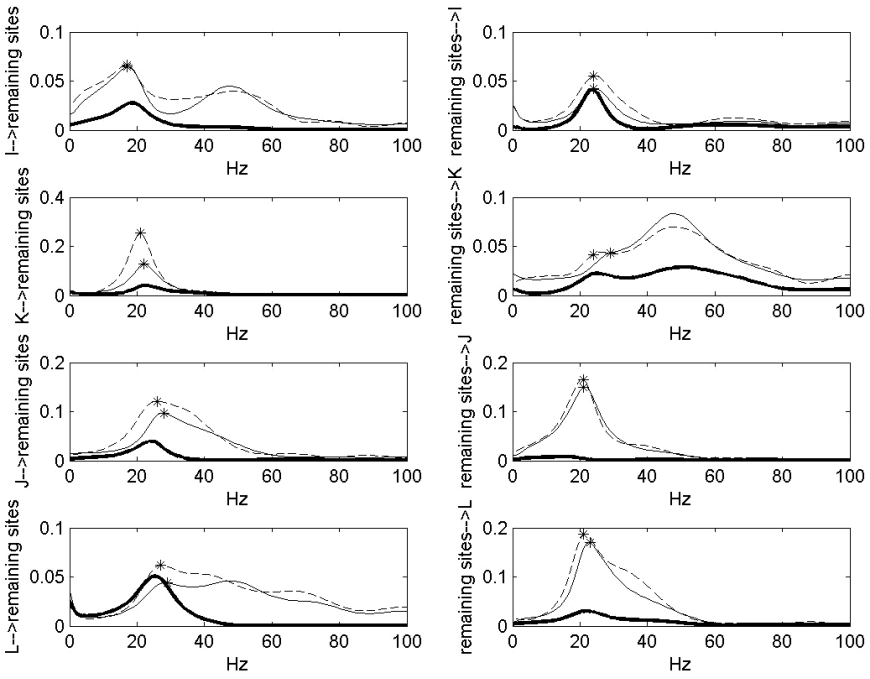

Fig. 3. Blockwise Granger causality (solid thin) and summed pairwise Granger causality (dashed) for the beta-coherent network of monkey LU. The axis labels have the same meaning as for Fig. 2. The stars indicate the peaks of the Granger causality spectra within the beta (14–30 Hz) frequency range. The solid thick curves are the Granger causality spectra estimated between the individual time series of one site and the average of the time series of the block of other sites.

within the block was obtained, pairwise Granger causality was estimated between the time series of interest and this average time series. Figure 3 shows that the level of Granger causality is not consistent with the other two methods for most recording sites. For example, this analysis shows that the outgoing casual influence from precentral site L in LU was greater than the incoming influence, in contrast to both the summed pairwise and the blockwise methods. Thus, this average method does not appear to be suitable for an accurate estimation of the causal relations between blocks. This is an additional proof that spatial averaging of cortical activity, typically used to ease computational burden and/or to filter out noise, may lead to erroneous results of analysis. From Figs. 2 and 3 one can also estimate the relative intensity of the outgoing to incoming Granger causality for each site. From the blockwise Granger causality method, the outgoing influence exerted by the primary somatosensory cortex site on the rest of the network is about five times larger than the incoming influence it receives from the network in monkey GE (site I), and about two times larger in monkey LU (site K). On the other hand, the outgoing blockwise Granger causality exerted by the precentral site on the rest of the network is about one fifth of the incoming influence that it receives from the network in monkey GE (site J) and about one third in monkey LU (site L). These results are consistent with the results of the pairwise Granger causality method reported by Brovelli *et al.*[10]

For a more quantitative comparison between the two methods, we estimated the frequency and amplitude of the peaks in the Granger causality spectra obtained by the pairwise and blockwise methods. The scatter plots in Fig. 4 display the combined results from both monkeys. The points in the top two panels represent peak amplitudes and peak frequencies of outgoing causal influence (i.e., Granger causality from one site to the rest of the network), and the bottom two panels represent peak amplitude and peak frequency of incoming causal influence (i.e., Granger causality from the rest of the network to the given site). As can be seen, the peak frequencies (left column) and peak amplitudes (right column) from the two methods are both highly correlated, indicating that the two methods give very similar results. The slopes of the linear regression line for the peak

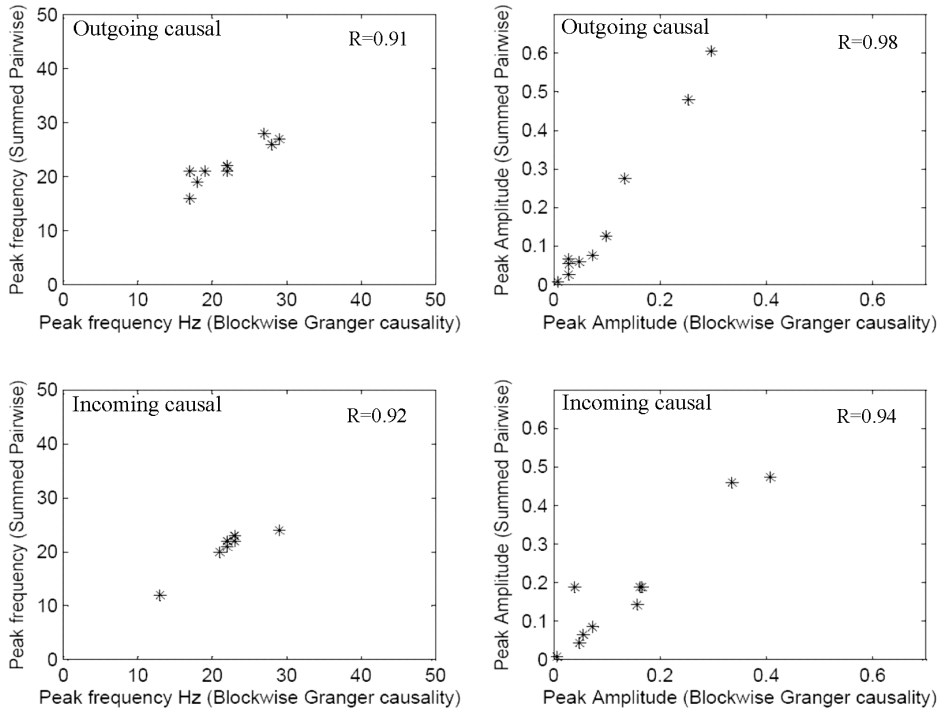

Fig. 4. Comparison of blockwise versus summed pairwise Granger causality methods. The results of the two methods are presented in scatter plots for frequency (left column) and amplitude (right column) of the peak Granger causality. Only peaks in the beta frequency band are considered here. The panels in the top row refer to the outgoing causal influence, and the panels in the bottom row refer to the incoming causal influence, from the point of view of the single time series block. Each panel is a composite of the results from both monkeys used in this study. Linear correlation coefficients are indicated on top of each figure.

amplitude scatter plots are both slightly larger than one, confirming the earlier observation that the peak amplitudes from the blockwise method tend to be smaller than the ones from the summed peak amplitudes by the pairwise method.

4. Discussion

For two blocks of time series, two methods can be used to assess the causal relations between them: pairwise method and blockwise method. The main result of this work on the analysis of multi-site cortical field potential time series is that the blockwise Granger causality method, which is based on a single MVAR model fitting to all available time series, provides an efficient and useful tool for investigating the causal relations between one site and a block of other sites in densely coupled networks such as the ones in the brain. A careful comparison shows that the two methods give consistent results. In general practice, it may be useful to combine the blockwise and pairwise approaches. For example, the blockwise method may be used first to identify important regions of interactions, and the pairwise method is then used to further assess the contributions of specific sites within and between those regions (network clustering). In medical applications, these methods may also be useful in the monitoring of systems that slowly move towards synchronization, for example, prior to the onset of epileptic seizures (see Ref. 15 for a review on this topic[15]). In this case, the driving site (or block of sites) and its dynamics may be identified through the causality analysis shown herein. Specifically, our methods might be useful for the identification of the epileptogenic zone as the block of sites that drive the rest of the brain into seizures. Nonetheless, it is important to note that in some situations, both the pairwise and blockwise methods may produce misleading results. Specifically, if the influence between two sites (or blocks) is not direct, but mediated by a third site (or block), neither the simpler pairwise nor blockwise analyses considered here are able to completely resolve the connectivity/causality pattern. Another method, called the

conditional Granger causality, has been developed to deal with this problem.[11,16]

Acknowledgements

This research was supported by MH071620 and MH064204. We thank the referees for helpful comments.

References

1. N. Wiener, The theory of prediction, in *EFBeckenbach Modern Mathermatics for Engineers* (ed.) (McGraw-Hill, New York, 1956).
2. C. W. J. Granger, Investigating causal relations by econometric models and cross-spectral methods, *Econometrica* **37**(3) (1969) 424–438.
3. J. Geweke, Measurement of linear-dependence and feedback between multiple time-series, *Journal of the American Statistical Association* **77**(378) (1982) 304–313.
4. R. Goebel, A. Roebroeck, D. S. Kim and E. Formisano, Investigating directed cortical interactions in time-resolved fMRI data using vector autoregressive modeling and Granger causality mapping, *Magnetic Resonance Imaging* **21**(10) (2003) 1251–1261.
5. C. Bernasconi, A. von Stein, C. Chiang and P. Konig, Bi-directional interactions between visual areas in the awake behaving cat, *Neuroreport* **11**(4) (2000) 689–692.
6. C. Bernasconi and P. Konig, On the directionality of cortical interactions studied by structural analysis of electrophysiological recordings, *Biological Cybernetics* **81**(3) (1999) 199–210.
7. M. Kaminski, M. Ding, W. A. Truccolo and S. L. Bressler, Evaluating causal relations in neural systems: Granger causality, directed transfer function and statistical assessment of significance, *Biological Cybernetics* **85**(2) (2001) 145–157.
8. A. Roebroeck, E. Formisano and R. Goebel, Mapping directed influence over the brain using Granger causality and fMRI, *Neuroimage* **25**(1) (2005) 230–242.
9. W. Hesse, E. Moller, M. Arnold and B. Schack, The use of time-variant EEG Granger causality for inspecting directed interdependencies of neural assemblies, *Journal of Neuroscience Methods* **124**(1) (2003) 27–44.
10. A. Brovelli, M. Ding, A. Ledberg, Y. Chen, R. Nakamura and S. L. Bressler, Beta oscillations in a large-scale sensorimotor cortical network: Directional influences revealed by Granger causality, *Proceedings of the National Academy of Sciences of the United States of America* **101**(26) (2004) 9849–9854.
11. Y. Chen, S. L. Bressler and M. Ding, Frequency decomposition of conditional Granger causality and application to multivariate neural field potential data, *Journal of Neuroscience Methods* **150**(2) (2006) 228–237.
12. C. Gourieroux and A. Monfort, *Time Series and Dynamic Models* (Cambridge University Press, London, 1997).
13. M. Ding, S. L. Bressler, W. Yang and H. Liang, Short-window spectral analysis of cortical event-related potentials by adaptive multivariate autoregressive modeling: Data preprocessing, model validation, and variability assessment, *Biol Cybern* **83**(1) (2000) 35–45.
14. S. L. Bressler, R. Coppola and R. Nakamura, Episodic multiregional cortical coherence at multiple frequencies during visual task-performance, *Nature* **366**(6451) (1993) 153–156.
15. L. D. Iasemidis, Epileptic seizure prediction and control, *IEEE Trans Biomed Eng* **50**(5) (2003) 549–558.
16. J. F. Geweke, Measures of conditional linear-dependence and feedback between time-series, *Journal of the American Statistical Association* **79**(388) (1984) 907–915.